

The slingshot effect: a possible new laser-driven high energy acceleration mechanism for electrons

Gaetano Fiore^{1,3}, Renato Fedele^{2,3}, Umberto de Angelis³,

¹ Dipartimento di Matematica e Applicazioni, Università di Napoli “Federico II”, 80126 Napoli, Italy

² Dipartimento di Fisica, Università di Napoli “Federico II”, 80126 Napoli, Italy

³ INFN, Sezione di Napoli, 80126 Napoli, Italy

We show that under appropriate conditions the impact of a very short and intense laser pulse onto a plasma causes the expulsion of surface electrons with high energy in the direction opposite to the one of propagation of the pulse. This is due to the combined effects of the ponderomotive force and the huge longitudinal field arising from charge separation (“slingshot effect”). The effect should also be present with other states of matter, provided the pulse is sufficiently intense to locally cause complete ionization. An experimental test seems to be feasible and, if confirmed, would provide a new extraction and acceleration mechanism for electrons, alternative to traditional radio-frequency-based or Laser-Wake-Field ones.

I. INTRODUCTION

Recently developed laser technologies have allowed the production of very intense and coherent electromagnetic (EM) waves concentrated in ultra-short pulses, whose interaction with matter is characterized by fast, huge and highly nonlinear effects. In particular, the very strong longitudinal ponderomotive forces caused by such laser pulses produces very large and very fast charge separations between ions and electrons and thereby very strong longitudinal electric fields (in matter other than plasma, this occurs after the huge kinetic energy transferred to the electrons has locally ionized matter into a plasma). In some conditions, a plasma wave with a phase velocity almost equal to the group velocity of the laser pulse appears behind the latter. This characterizes a mechanism known as Laser Wake Field (LWF) excitation [1–3], which can be used to accelerate beams of charged particles injected from outside (*external injection* [4]) or belonging to the plasma itself (*self injection* [5]).

In plasma-based acceleration schemes working with the external injection, lasers with power of up to hundreds of Terawatts are employed. Their typical intensity and pulse duration range from 10^{20} to 10^{22} Watt/cm² and from sub-pico to femto-seconds, respectively. In these conditions, the ponderomotive effect leads to extreme charge separation corresponding to the maximum electric field E_{max} that can be achieved in a plasma of a given unperturbed density. This is reached when the electron density perturbation becomes of the order of the equilibrium density n_0 and $E_{max}[\text{V/cm}] \approx \sqrt{n_0[\text{cm}^{-3}]}$. Then, for $n_0 \sim 10^{18} \text{ cm}^{-3}$, $E_{max} \sim 1 \text{ GV/cm}$. The ultra-strong acceleration gradients (compared to the maximum fields that are produced in the conventional accelerating machines based on radio-frequency cavities, which are of the order of tens MV/m) allow to reduce the length of the acceleration chamber of several orders of magnitude. Then, externally injected electrons could reach an energy of the order of a 1 GeV in a few centimeters. However, the acceleration of an externally injected beam is effective only if the initial velocity of the latter is close to the phase

velocity of the plasma wave (hence to the light speed c), so that the dragging action of the wake lasts sufficiently long. Therefore, acceleration machines based on external injection can be used only after some pre-acceleration stage.

With a very intense laser pulse, the plasma electrons reach very high energies in very short times. In the self injection scheme [5] the accelerated electrons are those which are naturally (albeit violently) ejected from the plasma itself. Actually, in the works of experimental feasibility, this second acceleration process, if compared to the external injection scheme, was not very efficient and reliable in terms of intensity, energy spread and collimation. Therefore, it appeared to be more suitable as an electron beam source and pre-acceleration device to be used before a subsequent acceleration stage, whether conventional or plasma-based. However, recent investigations [6, 7] have shown that acceleration schemes that are based on a violent laser-plasma interaction should work in a regime for which the laser pulse is strong enough to blow out electrons and leave a wake of immobile positively charged ions (*bubble regime* or *blowout regime*). Such a regime has been confirmed by several valuable particle-in-cell simulations. A bubble can both trap and accelerate the background electrons and it seems to be necessary to produce a very collimated, quasi-monoenergetic, self-injected electron beam. Bubbles are typically encircled by a return current that is created by relativistic electrons. However, a reliable quantitative description is still missing. Remarkably, a very recent experiment with self-injection has produced quasi-monoenergetic electrons with energy well beyond 1 GeV. By applying new Petawatt laser technology, a group of researchers of Texas University at Austin [8] was able to produce electron bunches with a spectrum prominently peaked at 2 GeV with only a few percent energy spread and unprecedented sub-milliradian divergence. This circumstance seems to characterize the signature of the bubble formation that is followed immediately by a strong localized injection.

In this paper, we show that a different acceleration

mechanism of plasma electrons may occur under suitable conditions for the pulse length, duration and shape. In the self injection scheme the plasma electrons are dragged in and ejected *forward*, whilst in this new *slingshot* mechanism *surface electrons* (i.e. plasma electrons in a thin layer just beyond the surface of the plasma) are expected to be expelled with high energy *backwards*. This means that, shortly after the impact of a suitable ultra-short and ultra-intense laser pulse in the form of a pancake normally onto a plasma, such electrons are expelled along the direction that is *opposite* to the one of the pulse propagation. The mechanism is very simple: the surface electrons first are given sufficient electric potential energy by displacement (through the ponderomotive force produced by the pulse) with respect to the ions, then are pulled back by the electric force exerted by the latter and the other electrons, and leave the plasma; provided the spot size is sufficiently small their energy will be enough to escape to infinity. The stages are schematically depicted in fig. 1. Below we show that the conditions for this to happen are that the pulse is sufficiently short, the radius R of the pancake is sufficiently small for the EM field inside the pulse to be sufficiently intense, but also relatively large to avoid trapping of the electrons. As this is based only on the interaction of the pulse with the first layer of plasma, a reliable, rather explicit magnetohydrodynamic description seems to be possible at least for a low density plasma. This is given here, referring the reader to [9] for the proof of some essential mathematical results (a summary can be found in [10]). The results are used to suggest possible experiments at the Italian INFN facility FLAME (Frascati Laser for Acceleration and Multidisciplinary Experiments) [11], and preliminary estimates for possible experiments at more powerful facilities like the Extreme Light Infrastructure (ELI) [12]. We expect that for higher density plasmas and suitably higher intensities of the EM field the slingshot effect still occurs and leads to the expulsion of higher energy electrons; a quantitative estimate of the latter is not possible by computations within the low density approximation considered in [9], and will be considered elsewhere.

It should be pointed out that the interaction of very intense laser radiation with the boundary of an *overdense* plasma has been studied in [13–15] using particle-in-cell simulations or (simplified) analytical models. It was found that the effect on the EM radiation (respectively transmission and reflection, absorption, conversion from incident femtosecond to reflected attosecond pulses) may be accompanied [13, 14] by (temporary or final) emission of nanobunches of electrons backwards; this is the result of a multi-cycle in-out acceleration process (described stochastically, when the hydrodynamic description fails) of the boundary electrons by a quasistationary EM wave. On the contrary, the acceleration process presented here is induced by a *short pulse* onto an *underdense* plasma and produces a *single* bunch of electrons after a unique forward acceleration followed by a unique backward one; moreover, our description is purely *hydrodynamic*.

II. THE MODEL

We describe the plasma as a fully relativistic collisionless fluid, with the “plasma + EM field” system fulfilling the Lorentz-Maxwell and the continuity equations. We assume that the plasma is initially neutral, unmagnetized and at rest with electron density equal to zero and to a constant n_0 respectively in the regions $z < 0$ and $z \geq 0$. We consider a purely transverse EM pulse in the form of a pancake with cylindrical symmetry around the z -axis, propagating in the positive \hat{z} direction and hitting the plasma surface at $t = 0$. Our simplified model of the impact leading to the slingshot effect consists of the following elements:

1. During the whole process we schematize the pancake pulse (see fig. 1-1) as a free plane pulse multiplied by the characteristic function of the cylinder C_R of equation $\rho^2 \equiv x^2 + y^2 \leq R^2$ (with some finite radius R)

$$\mathbf{E}^\perp(t, \mathbf{x}) = \boldsymbol{\epsilon}^\perp(ct - z)\theta(R - \rho), \quad \mathbf{B}^\perp(t, \mathbf{x}) = \hat{z} \wedge \boldsymbol{\epsilon}^\perp(ct - z)\theta(R - \rho) \quad (1)$$

($\mathbf{E}, \mathbf{B}, c, \theta$ respectively stand for the electric and magnetic field, the velocity of light, the Heaviside step function, and we use CGS units throughout the paper); the ‘pump’ function $\boldsymbol{\epsilon}^\perp(\xi)$ vanishes outside some finite interval $0 < \xi < l$. The pulse reaches the plasma surface $z = 0$ at $t = 0$. We justify (1) at the end of section IV.

2. We neglect the motion of ions (this is justified at the end of section III).

3. We first study (section II.1) the associated plane problem [$R = \infty$ in (1)] in a parameter range allowing simple approximations of the forward and backward motions of the surface electrons.

4. We determine (section II.2) a sufficiently large R such that the approximation 3. is satisfactory for the surface electrons within some inner cylinder C_r of equation $\rho^2 \leq r^2$, with $r \geq R/2$. We also estimate the corresponding deceleration of the electrons after expulsion and thus lower bounds for their number and final energy.

Items 1 ÷ 4 and the other used approximations (see section IV) make the effects of the model easily computable. Their justification consists in showing that their effect is either small or “conservative”, i.e. that it leads to *underestimate* the size of the slingshot effect. This is fine for the purpose of the present work, which is to give a safe theoretical basis to the prediction of this new effect, rather than to optimize it. Most proofs and detailed calculations are concentrated in the appendix.

Now some remarks on notation. We denote as $\mathbf{x}_e(t, \mathbf{X})$ the position at time t of the electrons’ fluid element initially located at $\mathbf{X} \equiv (X, Y, Z)$, and for each fixed t as $\mathbf{X}_e(t, \mathbf{x})$ the inverse. We denote as n_e, \mathbf{v}_e the electrons’ Eulerian density and velocity, and shall often use the dimensionless quantities $\boldsymbol{\beta}_e \equiv \mathbf{v}_e/c$, $\mathbf{u}_e \equiv \mathbf{p}_e/mc = \boldsymbol{\beta}_e/\sqrt{1 - \boldsymbol{\beta}_e^2}$, $\gamma_e \equiv 1/\sqrt{1 - \boldsymbol{\beta}_e^2} = \sqrt{1 + \mathbf{u}_e^2}$. The Lagrangian counterparts depend on t, \mathbf{X} , rather than on t, \mathbf{x} , and are denoted by a tilde, e.g. $\tilde{\mathbf{p}}^\perp(t, \mathbf{X}) = \tilde{\mathbf{p}}^\perp[t, \mathbf{x}_e(t, \mathbf{X})]$.

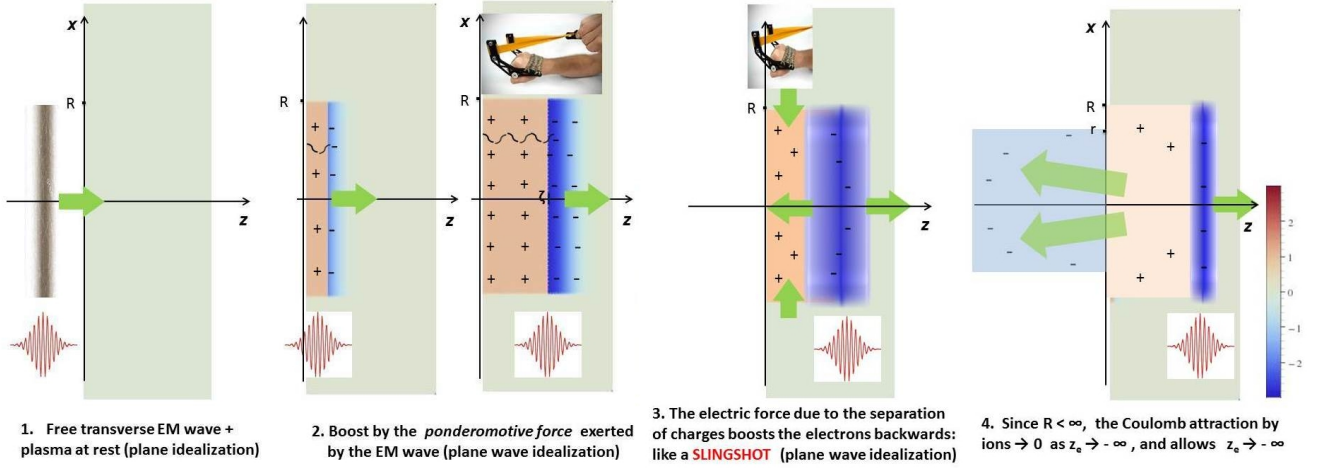


FIG. 1. Schematic stages of the slingshot effect

II.1. Plane wave idealization

For $R = \infty$ we choose the gauge so that the transverse (with respect to \hat{z}) vector potential is the physical observable $\mathbf{A}^+(t, z) = -\int_{-\infty}^t dt' c \mathbf{E}^+(t', z)$; then $\mathbf{B} = \mathbf{B}^+ = \hat{z} \wedge \partial_z \mathbf{A}^+$, $c \mathbf{E}^+ = -\partial_t \mathbf{A}^+$. By (1) it is $\mathbf{A}^+(t, z) = \boldsymbol{\alpha}^+(ct - z)$, where $\boldsymbol{\alpha}^+(\xi) \equiv -\int_{-\infty}^{\xi} d\xi' \boldsymbol{\epsilon}^+(\xi')$, implying $\boldsymbol{\alpha}^+(\xi) = 0$ for $\xi \leq 0$.

As known, the transverse component of the equation of motion $d\mathbf{p}_e/dt = -e(\mathbf{E} + \frac{\mathbf{v}}{c} \wedge \mathbf{B})$ of the electrons implies $\mathbf{p}_e^+ - \frac{e}{c} \mathbf{A}^+ = \text{const}$ on the trajectory of each electron; this is zero at $t = 0$, hence $\mathbf{p}_e^+ = m c \mathbf{v}_e^+ = \frac{e}{c} \mathbf{A}^+ = \frac{e}{c} \boldsymbol{\alpha}^+$. The longitudinal component involves the electric force $F_e^z \equiv -e E^z$ and the magnetic one

$$F_m^z \equiv -\frac{e}{c} (\mathbf{v}_e \wedge \mathbf{B})^z = \frac{-e^2}{2m c^3 \gamma_e} \partial_z \mathbf{A}^{+2} = \frac{e^2}{2m c^4 \gamma_e} \partial_t \boldsymbol{\alpha}^{+2}(ct - z).$$

Regarding ions as immobile, the Maxwell equations imply

$$E^z(t, z) = 4\pi n_0 e \{ z \theta(z) - Z_e(t, z) \theta[Z_e(t, z)] \}. \quad (2)$$

(see e.g. eq. (46) in [9]). The electric force $\widetilde{F}_e^z(t, Z) = -e \widetilde{E}^z(t, Z) = -e E^z[t, z_e(t, Z)]$ acting at time t on the electrons initially located at \mathbf{X} (with $Z \geq 0$) is therefore

$$\widetilde{F}_e^z(t, Z) = \begin{cases} -4\pi n_0 e^2 \Delta z_e \text{ (elastic force)} & \text{if } z_e > 0, \\ 4\pi n_0 e^2 Z \text{ (constant force)} & \text{if } z_e \leq 0, \end{cases} \quad (3)$$

where $\Delta z_e \equiv z_e(t, Z) - Z$ is the electron displacement with respect to its initial equilibrium position Z . \widetilde{F}_e^z is thus the force of a harmonic oscillator (with equilibrium at $z_e = Z$) in the bulk and a nonnegative constant outside.

Assume that $\boldsymbol{\epsilon}^+ = \epsilon_s \boldsymbol{\epsilon}_o^+$, where $\epsilon_s(\xi) \geq 0$ slowly varies inside the interval $0 < \xi < l$ and is zero outside, while $\boldsymbol{\epsilon}_o^+(\xi)$ sinusoidally oscillates around zero with a period $\lambda \ll l$. If the pump $\boldsymbol{\epsilon}^+$ is very large, by continuity we expect the EM field to remain close to the compact-support travelling-wave (1) also for small $t > 0$. In Ref. [9] it is

shown that this is indeed the case in the space-time region $0 \leq ct - z \leq \xi_0$, $0 \leq ct + z \ll \frac{2\pi}{K\lambda}$, where ξ_0 is the first maximum point of $\epsilon_s(\xi)$, and $K \equiv \pi e^2 n_0 / m c^2$.

The first effect of the impact of the pulse is to boost *all* the electrons reached not only in the x, y directions through the electric force $-e \mathbf{E}^+ = -e \boldsymbol{\epsilon}^+$, but also in the z direction through F_m^z . Since $\mathbf{p}_e^+ = \frac{e}{c} \boldsymbol{\alpha}^+$ oscillates about zero for $0 \leq \xi \leq l$, and $\boldsymbol{\alpha}^+(\xi) = \text{const} \simeq 0$ for $\xi \geq l$, then the transverse motion approximately averages to zero, and $\mathbf{p}_e^+ \simeq 0$ after the pulse. Since $\boldsymbol{\alpha}^{+2}$ is zero at the front of the pulse and positive inside, its time derivative is positive at the front; hence the initial z -boost is necessarily *positive*. Because of this boost, the first layer of ions remains unshielded while electrons accumulate just beyond the surface $S_0(t)$ of discontinuity of n_e delimiting the $Z = 0$ surface electrons [the resulting charge distribution in the approximation (A9) to be considered here is depicted in the first four upper pictures of fig. 8]. This charge separation generates the *slingshot*, *i.e.* the longitudinal electric force \widetilde{F}_e^z pushing the boosted electrons backwards. If the time scale of significant variations of ϵ_s (and the duration l/c of the pulse, *a fortiori*) is much larger than the characteristic period $\tau \gtrsim T_H^{nr}$ of oscillation of the electrons ($T_H^{nr} \equiv \sqrt{\pi m / n_0 e^2} = 2\pi / \omega_p$ is the period of the corresponding nonrelativistic harmonic oscillator) [16], then the electrons do many oscillations during the pulse, the power $P \equiv \widetilde{F}_m^z \widetilde{v}^z$ transferred by the magnetic force to each electron oscillates about zero, and its time integral \mathcal{E}_p (the transferred energy, or *slingshot loading*) is approximately zero. This was the situation normally encountered in laboratories until a few years ago, because of the inability to generate sufficiently low densities and short pulses. If $l/c < T_H^{nr}/4$, then \widetilde{v}^z is positive during all the pulse while \widetilde{F}_m^z oscillates about zero, and overall we obtain only a moderate slingshot loading $\mathcal{E}_p > 0$ (if $l/c \ll T_H^{nr}$ a good approximation of the motion is the zero-density solution recalled below). Therefore to increase \mathcal{E}_p

we study the range $l/c \sim T_H^{nr}$. Denoting as $\langle \rangle$ the average over a period λ , we find $F_p^z \equiv \langle F_m^z \rangle \propto \partial_t \epsilon_s^2(ct-z)$, and the ponderomotive force F_p^z is respectively positive, negative when ϵ_s^2 is strictly increasing, decreasing - as known. If for simplicity $\epsilon_s^2(\xi)$ has a unique maximum point ξ_0 , to maximize \mathcal{E}_p we should make \tilde{v}^z switch from positive to negative only once during the pulse, exactly at the time \bar{t} when the maximum reaches the electrons, so that $\langle P \rangle \simeq F_p^z \tilde{v}^z$ keeps nonnegative during all the motion. This can be achieved by tuning n_0 and the pulse length in the range

$$l \sim cT_H^{nr}/2 = \sqrt{\pi m c^2 / 4n_0 e^2}, \quad (4)$$

as well as the shape of the pulse [17]. After overcoming the surface electrons, the EM pulse will further propagate forward, slowly damped; it may also generate a wake with deeper electrons in the plasma. We shall ignore such phenomena and follow only the motion of the surface electrons, showing that a thin layer is finally expelled with high energy in the backward direction.

The above picture is confirmed by the first steps of an iterative resolution scheme of the plane problem proposed in [9]. The initial step is the ‘zero-density’ solution, which we summarize in eq. (A1-A3). According to it, the longitudinal motion of any electron is never backward. The $Z=0$ electrons are reached by the maximum of ϵ_s^2 at time $t_0 = \Xi_e(\xi_0)/c$, where Ξ_e is defined in (A4). The error with respect to the real solution increases with t . In the second step (first correction to the ‘zero-density’ motion) these electrons invert their motion at a time \bar{t}_1 given in subsection A. Electrons initially located at small $Z > 0$ will approximately move in the same way, after the space-time displacement ($Z, Z/c$). For technical simplicity in this work we stick to parameters in a range [see conditions (A6) and the paragraph of eq. (A7)] such that the relative difference between the zero-density and the first corrected motion keeps much smaller than 1 for $t \leq t_0$ and rapidly grows for $t > t_0$, so that $\bar{t}_1 - t_0$ is positive, but as small as possible. This ensures [9] that: i) the ‘zero-density’ motion (A1-A2) is a good approximation of the real forward motion for all electrons initially located in a thin superficial layer, in particular it can be used to estimate their maximal displacement ζ :

$$\zeta \simeq Y_e^z(\xi_0), \quad Y_e^z(\xi) \equiv \frac{e^2}{2m^2 c^4} \int_0^\xi dy \alpha^{+2}(y); \quad (5)$$

ii) in this approximation the slingshot loading is efficient.

In the backward motion of the surface electrons for simplicity we underestimate as $\widetilde{F}_e^z(t, Z)$ the longitudinal force, neglecting the backward \widetilde{F}_m^z due to the last part of the pulse and of the generated ‘reflected’ EM wave (see the final section). We denote the potential energy associated to the conservative force $F_e^z(z_e, Z) \equiv 4\pi e^2 n_0 [Z - z_e \theta(z_e)]$ of (3) as [18]

$$U(z_e, Z) = 2\pi n_0 e^2 [\theta(z_e) z_e^2 - 2z_e Z + Z^2]. \quad (6)$$

In fig. 2-left we plot $f \equiv F_e^z/4\pi e^2 n_0$ and $u \equiv U/2\pi e^2 n_0$ as functions of z_e for a few values of $Z \geq 0$. Using energy conservation during the backward motion

$$H \equiv mc^2 \gamma_e(z_e, Z) + U(z_e, Z) = mc^2 \sqrt{1 + \mathbf{u}_{ei}^{+2}} + 2\pi n_0 e^2 \zeta^2 \geq mc^2 + 2\pi n_0 e^2 \zeta^2, \quad (7)$$

one can compute $\gamma_e \equiv 1/\sqrt{1 - \mathbf{v}_e^2/c^2}$, and therefore also β_e^z , as functions of z_e, Z (here $m c \mathbf{u}_{ei}^+$ is the electron transverse momentum when the displacement is maximal, $z_e - Z = \zeta$), and the longitudinal motion by quadrature (appendix A); the combined forward-backward motion is summarized in eq. (A9) and plot in fig. 7 for some fixed, relevant values of the parameters and a few different values of Z (see below); as the corresponding map $Z \mapsto z$ is one-to-one for all t , different worldlines do not intersect. This shows that in this time lapse our treatment of the electron fluid as collisionless is consistent. The mechanical energy of the $Z=0$ electrons after expulsion ($z_e < 0$) is purely kinetic, because $U(z_e, 0) = 0$. However, as $U(-\infty, Z) = \infty$ for $Z > 0$, one concludes that in the $R = \infty$ idealization only the former electrons escape to $z_e = -\infty$ infinity; inner electrons invert their motion where γ_e reaches its minimum $\simeq 1$ and then oscillate around Z . We now show that $R < \infty$ allows the escape of a thin layer of electrons.

II.2. Inclusion of 3D-effects

In the realistic case of a finite radius R the ponderomotive force of the pulse will boost only the electrons approximately in the cylinder C_R of the same radius. We require R to be sufficiently large with respect to ζ in order that: i) the electrons in a cylinder C_r of radius $r > 0$ undergo approximately the same motion (A9) as with $R = \infty$; ii) there is no trapping, i.e. the way backwards out for the surface electrons within C_r is not obstructed by the electrons initially located just outside the lateral surface ∂C_R of C_R (the latter electrons first are boosted outward, because on ∂C_R so is directed the gradient of \mathbf{E}^{+2} of the pulse, then move towards the z -axis attracted by the ions). At the end of appendix B we show that both requirements are satisfied by the condition

$$R \gtrsim \sigma \zeta, \quad (8)$$

with σ a little larger than 1 (at least in the range of relevant conditions). We now show that: iii) due to the finite R , outside the bulk the attracting force by the ions decreases sufficiently fast with $|z_e|$ to allow a thin layer of the expelled electrons to escape to infinity.

As said $\widetilde{\mathbf{p}}_e^- \simeq 0$ after the pulse. We consider only the motion of the electrons moving along the \bar{z} -axis ($\rho = 0$) after the pulse; in other words we consider those electrons which experience the strongest restoring force after expulsion, by symmetry reasons. In fig. 3-up we depict the expected charge distribution of the electrons initially

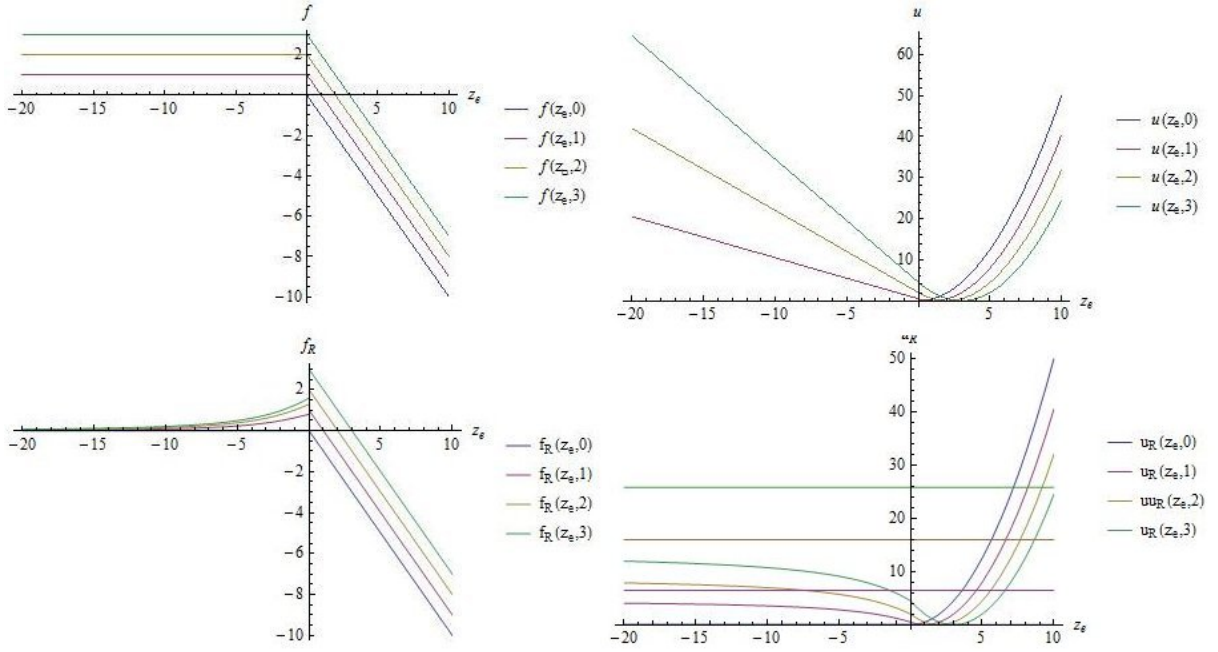


FIG. 2. The rescaled longitudinal electric force f (left, up) and the associated rescaled potential energy u (left, down) in the idealized plane wave case, the rescaled longitudinal electric force f_R (right, up) and the associated rescaled potential energy u_R (right, down) in the case of a pancake of radius $R = 5$, plotted as functions of z_e for $Z = 0, 1, 2, 3$; the horizontal lines in the right down graph are the left asymptotes of u for $Z = 0, 1, 2, 3$.

located at $Z \gtrsim 0$ at a time t shortly after their expulsion. The light blue area is occupied only by electrons. The left border, the dashed line and the solid line respectively represent the surfaces S_0, S_1, S_2 occupied by the electrons initially located at the points $\mathbf{X}' \in C_r$ such that $Z' = 0, Z, 2Z$. The orange area is positively charged due to an excess of ions. We can bound the *real* electric longitudinal force $\widetilde{F}_{e^{zr}}$ experienced by the electrons moving along the \bar{z} -axis as follows:

$$0 \leq \widetilde{F}_{e^{zr}}(t, Z) = -e\widetilde{E}_-^z(t, Z) - e\widetilde{E}_+^z(t, Z) \leq F_{eR}^z[z_e(t, Z), Z]. \quad (9)$$

Here $\widetilde{E}_-^z(t, Z)$ stands for the part of the longitudinal electric field generated by the electrons between S_0, S_2 ; since those between S_0, S_1 have by construction the same charge as those between S_1, S_2 , but are more dispersed, it will be $-e\widetilde{E}_-^z(t, Z) \leq 0$. The part $-e\widetilde{E}_+^z(t, Z)$ of the longitudinal electric force generated by the ions and the remaining electrons (at the right of S_2) will be smaller than the force F_{eR}^z generated by the charge distribution depicted in fig. 3-down, where the remaining electrons are located farther from $(0, 0, z_e)$ (not in their actual positions, but in their initial ones \mathbf{X}') and therefore generate a smaller repulsive force. Using cylindrical coordinates (Z', ρ', φ') for \mathbf{X}' one easily finds for $z_e \leq 0$

$$\begin{aligned} F_{eR}^z(z_e, Z) &\equiv \int_0^{2Z} dZ' \int_0^R d\rho' \frac{2\pi n_0 e^2 \rho' (Z' - z_e)}{[\rho'^2 + (Z' - z_e)^2]^{3/2}} \\ &= 2\pi n_0 e^2 \left[2Z + \sqrt{z_e^2 + R^2} - \sqrt{(2Z - z_e)^2 + R^2} \right]. \end{aligned}$$

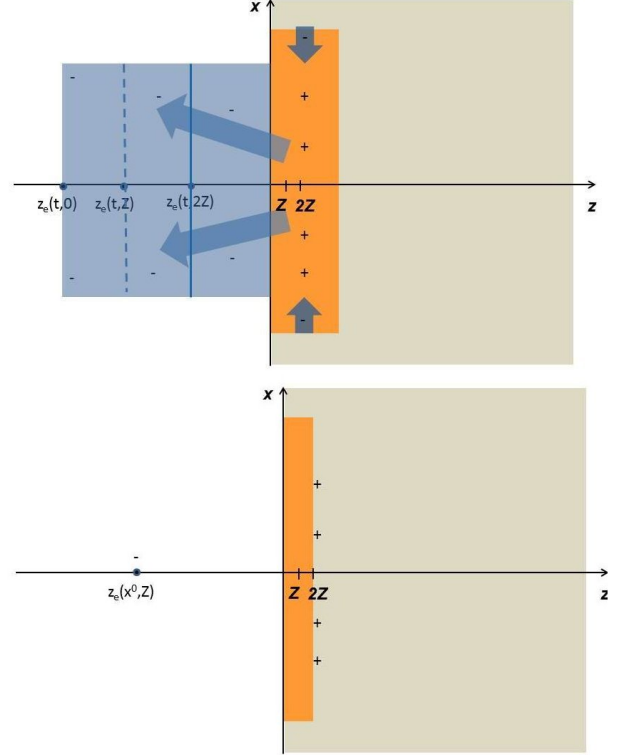


FIG. 3. Up: schematic picture of the expected charge distribution shortly after the expulsion (long arrows) of surface electrons; short arrows represent the inward motion of lateral electrons. Down: simplified charge distribution.

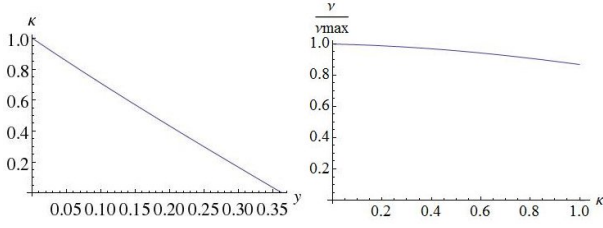


FIG. 4. $\kappa(y)$ vs. $y \in [0, y_M]$ ($y_M \equiv Z_M/\zeta$) (left), and the kinetic energy spectrum $\nu(\kappa)$ [in units of $\nu_{max} = \nu(\kappa=1)$] vs. $\kappa \in [0, 1]$ (right), for $R=1.5\zeta$.

F_{eR}^z is nonnegative and goes to zero as $z_e \rightarrow -\infty$, as it must be; it becomes a function of t through $z_e(t, Z)$ only. The associated potential energy is [19]

$$U_R(z_e, Z) = \pi n_0 e^2 \left[(z_e - 2Z) \sqrt{(z_e - 2Z)^2 + R^2} - 4Z z_e + R^2 \sinh^{-1} \frac{z_e - 2Z}{R} - z_e \sqrt{z_e^2 + R^2} - R^2 \sinh^{-1} \frac{z_e}{R} + 2Z^2 + 2Z \sqrt{4Z^2 + R^2} + R^2 \sinh^{-1} \frac{2Z}{R} \right],$$

a decreasing function of z_e with finite left asymptotes for any $Z \geq 0$. In fig. 2-right the plots of $f_R \equiv F_{eR}^z/4\pi n_0 e^2$, $u_R \equiv U_R/2\pi n_0 e^2$ replace those of f, u for $z_e \leq 0$. Denote as

$$\gamma_e^\infty(Z) = 1 + [2\pi n_0 e^2 \zeta^2 - U_R(-\infty, Z)]/mc^2 \quad (10)$$

$$= 1 + K [2\zeta^2 + 2Z^2 - 2Z \sqrt{4Z^2 + R^2} - R^2 \sinh^{-1} \frac{2Z}{R}]$$

the $z_e \rightarrow -\infty$ limit of the relativistic factor γ_e determined by replacing U by U_R with $\mathbf{u}_{ei}^{+2} = 0$ in (7), and as Z_M the value of Z for which $\gamma_e^\infty(Z) = 1$. As said, by such a replacement we overestimate the restoring rightwards force experienced by the electrons for $z_e < 0$. Consequently, the real relativistic factor of the electrons will be larger than the above γ_e , and the $M_0 \equiv \pi r^2 Z_M n_0$ electrons in C_r with $0 \leq Z \leq Z_M$ will be only part of those escaping to infinity; a lower bound for their final relativistic factor is $\gamma_e^\infty(Z)$. We find also the bound $|Q| \geq e\pi n_0 r^2 Z_M$ for the total expelled electric charge Q . In fig. 4-left we plot the normalized kinetic energy $\kappa \equiv [\gamma_e^\infty - 1]/2K\zeta^2$ as a function of $y \equiv Z/\zeta$ for $R=1.5\zeta$ (by definition $0 \leq \kappa \leq 1$, $0 \leq y \leq y_M$, where $y_M \equiv Z_M/\zeta$). The plot for $R=1.25\zeta$ does not differ significantly. The fraction of expelled electrons with initial position $Z' \in [Z, Z+dZ]$ is no less than $\pi r^2 n_0 dZ = \pi r^2 \zeta n_0 dy$ and, using γ_e^∞ instead of the real final relativistic factor, the fraction with kinetic energy in the interval $[\kappa, \kappa+d\kappa]$ is no less than $\nu(\kappa)d\kappa$, where

$$\nu(\kappa) = - \frac{\pi r^2 \zeta n_0}{\kappa'(y)|_{y=\hat{y}(\kappa)}} = \frac{\pi r^2 \zeta n_0}{2[\sqrt{4\hat{y}^2 + R^2/\zeta^2} - \hat{y}]_{y=\hat{y}(\kappa)}} \quad (11)$$

$[\hat{y}(\kappa)$ is the inverse of $\kappa(y)]$ represents the associated energy spectrum; this is plotted in fig. 4 right. By (10) the final relativistic factor of the expelled electrons is

$$\gamma_{eM} \equiv \gamma_e^\infty(0) \simeq 1 + 2K\zeta^2 \simeq 1 + 2K [Y_e^z(\xi_0)]^2; \quad (12)$$

the last \simeq holds under condition (A6).

We expect ζ, γ_{eM} to grow with the intensity - although at a slower rate - even if (A6) is not fulfilled.

III. EXPERIMENTAL FEASIBILITY

We now briefly discuss the experimental conditions for the slingshot effect, in particular for possible experiments at the FLAME facility in Frascati (but several other laboratories have comparable lasers) and at future ELI infrastructures. Laser pulses of wavelength λ , length $l \gg \lambda$, for simplicity symmetric around $\xi_0 = l/2$, concentrated onto an area πR^2 , have an energy

$$\mathcal{E} = \int dV \frac{\mathbf{E}^{\perp 2} + \mathbf{B}^{\perp 2}}{8\pi} \simeq \frac{(\pi R)^2}{\lambda^2} \int_0^l d\xi \mathbf{A}^{\perp 2} = \frac{4(\pi m c^2 R)^2}{(e\lambda)^2} Y_e^z(\xi_0). \quad (13)$$

(we have used the relation $\mathbf{E}^\perp \simeq \mathbf{A}^\perp 2\pi/\lambda$, valid for a modulated approximately monochromatic plane wave). By (5) $\zeta \simeq \mathcal{E}(e\lambda)^2/4(m\pi c^2 R)^2$, and (8) takes the form

$$R^3 \gtrsim \frac{\sigma \mathcal{E}(e\lambda)^2}{4(\pi m c^2)^2}$$

To maximize ζ and γ_{eM} we choose $R = \sigma\zeta$; we obtain

$$\sigma\zeta = R = \left[\frac{\sigma \mathcal{E}(e\lambda)^2}{4(\pi m c^2)^2} \right]^{\frac{1}{3}}. \quad (14)$$

The laser at the FLAME facility can shoot linearly polarized pulses with $\lambda \simeq 8 \times 10^{-5}$ cm, energy $\mathcal{E} = 5 \times 10^7$ erg, and an approximately gaussian modulating amplitude with width at half height $l' \simeq 7.5 \times 10^{-4}$ cm [11, 20]. In the appendix we show that it is sufficient to choose $\sigma \equiv R/\zeta = 1.25, 1.5$ to obtain the expulsion of the electrons in the corresponding layer $0 \leq Z \leq Z_M$ within a cylinder C_r of radius $r \geq R/2, 2R/3$ respectively. By (5), (14) $\sigma = 1.25$ gives $\zeta \simeq Y_e^z(\xi_0) \simeq 1.2 \times 10^{-3}$ cm, $R \simeq 1.5 \times 10^{-3}$ cm, whereas $\sigma = 1.5$ gives $\zeta \simeq Y_e^z(\xi_0) \simeq 1.07 \times 10^{-3}$ cm, $R \simeq 1.61 \times 10^{-3}$ cm. A plasma with $n_0 \geq 10^{17}$ cm $^{-3}$ is obtained by ionization from an ultracold gas (typically, helium) jet in a vacuum chamber hit by such an energetic laser pulse as soon as the Keldysh parameters $\Gamma_i \equiv \sqrt{U_i/k} = \sqrt{2U_i/mc^2 u_e^{\perp 2}}$ for both first and second ionization become smaller than 1; here k is kinetic energy, and the potentials U_i for first and second ionization are about 24eV, 54eV respectively. The length of the z -interval where both $\Gamma_i < 1$ plays the role of pulse length l . The ionization is practically complete and immediate if $R \lesssim 13 \times 10^{-3}$ cm, because for such field intensities the Keldysh parameter for double ionization reaches values $\Gamma_i^d < 1/100 \ll 1$ [20, 21] very fast. In [9] it has been shown that the model predicts no significant difference if the modulating amplitude ϵ_s is not chosen as a gaussian (blue curve in fig. 5) but rather inside the support $0 \leq \xi \leq l_p$ as the following fourth degree polynomial

$$\epsilon_s(\xi) = b_p \left[\frac{1}{4} - \left(\frac{\xi}{l_p} - \frac{1}{2} \right)^2 \right]^2 \theta \left[\frac{1}{4} - \left(\frac{\xi}{l_p} - \frac{1}{2} \right)^2 \right] \quad (15)$$

(purple curve in fig. 5), provided b_p, l_p are chosen so that the widths at half height of ϵ_s^2 and the pulse energy are the same; this gives $l_p \simeq 18.75 \times 10^{-4}$ cm, corresponding

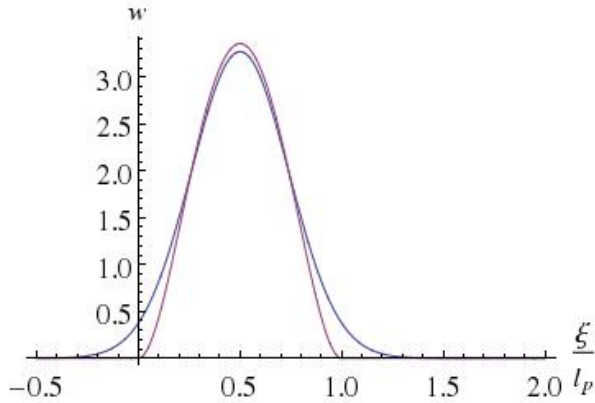


FIG. 5. Graphs of Gaussian (blue curve) and corresponding cut-off polynomial (15) (purple curve) normalized modulating amplitude $w(\xi) \equiv \frac{e\lambda}{2\pi mc^2} \epsilon_s(\xi)$.

to a pulse duration of about 6.25×10^{-14} s. We use such polynomial modulating amplitude (15) rather than the Gaussian one to make numerical computations easier.

We adopt $K = 2l_p^{-2}$ as maximal K . This, replaced in the definition of $T(\xi)$, gives $T(\xi_0) = 0.2$ and $T(\xi_0) = 0.19$ if $\sigma \equiv R/\zeta = 1.25$, $\sigma \equiv R/\zeta = 1.5$ respectively; both fulfill (A6)₂. So we adopt $K = 2l_p^{-2}$ as maximal K . Eq. (10) gives $Z_M \simeq 0.44\zeta$, $Z_M \simeq 0.36\zeta$; by (5), also condition (A6)₁ is fulfilled in either case. The time \bar{t}_1 of inversion of the motion is very close to t_0 in either case.

In the central, right columns of table I we summarize these and other outputs respectively for $R/\zeta = 1.25, 1.5$.

As $n_0 \ll n_c = \pi mc^2/e^2\lambda^2 \simeq 1.7 \times 10^{21} \text{cm}^{-3}$ (n_c is the critical density), we are indeed dealing with an underdense plasma. The pre-condition (4) for an efficient slingshot loading is fulfilled (the right-hand side $\pi/2\sqrt{K} \simeq 21 \times 10^{-4} \text{cm}$ is indeed of the order of the left-hand side). The maximal penetration ζ_i of the ions induced by the laser pulse is obtained from (5) replacing m with their mass, hence $\zeta_i \ll \zeta$; similarly, the displacement of ions due to their mutual electric repulsion is much smaller than that of the lateral electrons (see appendix B). This justifies the description of ions as immobile.

IV. CONCLUSIONS AND FINAL REMARKS

We have shown that the slingshot effect is possible if the laser pulse pancake is sufficiently short [eq. (4) and estimate after (A7)], its radius is not too small [eq. (8)], and the electromagnetic field inside is sufficiently intense for the expelled electrons to have a significant kinetic energy, i.e. a non-negligible $\gamma_{eM} - 1$. To make the latter condition quantitative and deduce conservative estimates of the final energy of the expelled electrons, as well as of the corresponding spectrum, we have used eq. (10), (12), (13), fig. 4, and assumed in addition the technical condition (A6).

	$R/\zeta = 1.25$	$R/\zeta = 1.5$
pulse energy \mathcal{E}	$\simeq 5 \text{ J}$	$\simeq 5 \text{ J}$
wavelength λ	$\simeq 8 \times 10^{-5} \text{ cm}$	$\simeq 8 \times 10^{-5} \text{ cm}$
pulse length l_p	$\simeq 18.75 \times 10^{-4} \text{ cm}$	$\simeq 18.75 \times 10^{-4} \text{ cm}$
pulse spot radius R	$= 1.5 \times 10^{-3} \text{ cm}$	$= 1.61 \times 10^{-3} \text{ cm}$
Kl_p^2	$= 2$	$= 2$
initial electron density n_0	$= 6.4 \times 10^{17} \text{ cm}^{-3}$	$= 6.4 \times 10^{17} \text{ cm}^{-3}$
electrons' penetration ζ	$\simeq 1.2 \times 10^{-3} \text{ cm}$	$\simeq 1.07 \times 10^{-3} \text{ cm}$
time \bar{t} of maximal penetration	$\simeq 7.15 \times 10^{-14} \text{ s}$	$\simeq 6.70 \times 10^{-14} \text{ s}$
time lapse of comeback $T_H/4$	$\simeq 5.247 \times 10^{-14} \text{ s}$	$\simeq 4.919 \times 10^{-14} \text{ s}$
time of expulsion t_e	$\simeq 1.24 \times 10^{-13} \text{ s}$	$\simeq 1.162 \times 10^{-13} \text{ s}$
expelled layer thickness Z_M	$\simeq 0.44\zeta$	$\simeq 0.36\zeta$
expelled electrons charge $ Q $	$\geq 1.41 \times 10^{-10} \text{ C}$	$\geq 1.44 \times 10^{-10} \text{ C}$
maximal relativistic factor γ_{eM}	$\simeq 1.83$	$\simeq 1.65$
maximal expulsion energy H	$\simeq 0.94 \text{ MeV}$	$\simeq 0.85 \text{ MeV}$
maximal electric field E_M^z	$\simeq 1.4 \text{ GV/cm}$	$\simeq 1.25 \text{ GV/cm}$

TABLE I. Main inputs and outputs for FLAME experiments

Eq. (A6)₁ in particular fixes an upper bound for K , hence for n_0 . If we keep R, ζ fixed and decrease n_0 then (A6)₁ still holds and by (12) $\gamma_{eM} - 1$ decreases proportionally. This scaling and the backward direction of expulsion may experimentally discriminate the slingshot effect from LWF or other acceleration mechanisms [22].

On the other hand, we expect that we can increase γ_{eM} by decreasing R and increasing n_0 so that ζ also decreases and (8) remains fulfilled. As this would violate the technical [9] condition (A6), a quantitative estimate of the corresponding slingshot effect is not possible at the level of approximation described here. Preliminary numerical computations at the next level indicate that the final kinetic energy of expelled electrons can be thus increased by at least one order of magnitude. This will be elaborated elsewhere.

The use of more powerful and shorter laser pulses would further increase the final energy of expelled electrons, while allowing the use of light solids as targets instead of gas jets. This could be accomplished, for instance, by the laser at the ELI facility, which will be able to shoot linearly polarized pulses with $\lambda \simeq 8 \times 10^{-5} \text{ cm}$, energy $\mathcal{E} \simeq 10^9 \text{ erg}$ and an approximately gaussian modulating amplitude with width at half height $l' \simeq 3 \times 10^{-4} \text{ cm}$ [12]. Preliminary estimates seem to show that use of such a laser would allow to further increase the final energy of expelled electrons by more than one order of magnitude.

In the present model we have done a number of approximations. In addition to the ones already mentioned, we have also neglected the negative ponderomotive force of the pulse after its maximum has overcome the electrons, as well as the negative ponderomotive force of the 'reflected EM wave' generated by the impact of the pulse on the plasma; both add to the electrostatic force to in-

crease the energy of the electrons in the expulsion phase. We have also approximated the transition region from $n_e=0$ to $n_e=n_0$ as the surface $z=0$, rather than a thin layer; we expect that the latter would modify the shape of the spectrum in fig. 4, but not the main results.

In (1) we have schematized the ρ -dependence of the pulse by $\theta(R-\rho)$, rather than by a more realistic smoothly decaying factor, such as $e^{-\rho^2/r^2(t)}$ with $r(0)\sim R$. Identifying $r(t)$ with R is justified during the impact because $\zeta, Z_M \ll l_R$ (the Rayleigh length of the focalized laser pulse at FLAME is $l_R \sim 2 \times 10^{-2}$ cm). The rather coarse approximation of a gaussian by a step function is adopted to ease the computations of the finite R corrections (appendix B) and is a further reason why our prediction of the expelled charge Q is an *underestimate* of the real one.

We have adopted all the described conservative estimates to give a safe basis to the prediction of this new effect, leaving optimization of the process as a task for further theoretical and experimental works.

ACKNOWLEDGMENTS

We thank L. Gizzi for information on FLAME and valuable suggestions, S. De Nicola for discussions. This work was partially supported by UniNA and Compagnia San Paolo under the grant "STAR Program 2013".

Appendix A: Plane plasma equations

Some results of [9]. Let $\widetilde{n}_{e0}(Z) \equiv n_e(0, Z)$ be the initial density. In the $\widetilde{n}_{e0} \equiv 0$ limit the electron motion in terms of the pump $\mathbf{A}^\perp(x) = \boldsymbol{\alpha}^\perp(ct-z)$ is:

$$\mathbf{u}_e^\perp(t, z) = \frac{e\boldsymbol{\alpha}^\perp(ct-z)}{mc^2}, \quad u_e^z = \frac{1}{2}\mathbf{u}_e^{\perp 2}, \quad \gamma_e = 1 + u_e^z, \quad (\text{A1})$$

$$\begin{aligned} z_e(t, Z) &= ct - \Xi_e^{-1}(ct - Z), \\ Z_e(t, z) &= ct - \Xi_e(ct - z) = z - Y_e^z(ct - z), \end{aligned} \quad (\text{A2})$$

$$\mathbf{x}_e^\perp(t, \mathbf{X}) = \mathbf{X}^\perp + \mathbf{Y}_e^\perp[ct - z_e(t, Z)],$$

$$\mathbf{X}_e^\perp(t, \mathbf{x}) = \mathbf{x}^\perp - \mathbf{Y}_e^\perp(ct - z),$$

$$\partial_t Z_e = -cu_e^z, \quad \partial_z Z_e = \gamma_e, \quad \partial_Z z_e = 1/\tilde{\gamma}_e. \quad (\text{A3})$$

Relations (A1) describe in the Eulerian picture forward travelling-waves moving with phase velocity equal to c . In (A2) we have used the primitives of \mathbf{u}_e, γ_e

$$\mathbf{Y}_e(\xi) \equiv \int_0^\xi dy \mathbf{u}_e(y), \quad \Xi_e(\xi) \equiv \int_0^\xi dy \gamma_e(y) = \xi + Y_e^z(\xi). \quad (\text{A4})$$

As $u_e^z \geq 0$, $Y_e^z(\xi)$ is increasing, $\Xi_e(\xi)$ is strictly increasing (and invertible), and the longitudinal motion is purely forward. Replacing (A3) in the relations

$$\begin{aligned} n_e(t, z) &= \widetilde{n}_{e0}[Z_e(t, z)] \partial_z Z_e(t, z), \\ \widetilde{n}_{e0}[Z_e(t, z)] \partial_t Z_e(t, z) &+ [n_e v_e^z](t, z) = 0. \end{aligned} \quad (\text{A5})$$

one obtains the Eulerian electron density in the next approximation. As said, here we assume $\widetilde{n}_{e0}(Z) = n_0 \theta(Z)$.

In Ref. [9] it is shown that the EM field remains close to the pump in the space-time region $0 \leq ct - z \leq \xi_0$, $0 \leq ct + z \ll \frac{2\pi}{K\lambda}$, and that the motion (A1-A4) is a good approximation of the real forward motion of all electrons with initial positions such that $0 \leq Z \leq Z_M$, provided [9]

$$\xi_0 + 2Y_e^z(\xi_0) + 2Z_M \ll \frac{2\pi}{K\lambda}, \quad T(\xi_0) \ll 1,$$

$$\text{where } V(\xi) \equiv \int_0^\xi dy Y_e^z(y), \quad (\text{A6})$$

$$G(\xi) \equiv \int_0^\xi dy \frac{(1+u_e^z)[e^{8KV}-1]}{1+u_e^z+e^{8KV}}(y), \quad T \equiv G/Y_e^z.$$

$T(\xi_0)$ gives the relative error between $Y_e^z(\xi_0)$ and ζ in the next approximation.

According to formulae (33) and (61) of [9], in the next approximation the time when the surface electron invert their motion is $\bar{t}_1 = \Xi_e(\xi_1)/c$, where ξ_1 is determined by $\exp[8KV(\xi_1)] = 1 + \eta[e\lambda\epsilon_s(\xi_1)/2\pi mc^2]^2$ $\eta = 1, 1/2$ respectively for circular, linear polarization) as a function of the physically tunable parameter K (or, equivalently, of n_0). This equation can be solved for K :

$$K(\xi_1) = \ln \{1 + \eta [e\lambda\epsilon_s(\xi_1)/2\pi mc^2]^2\} / 8V(\xi_1) \quad (\text{A7})$$

$[K(\xi_1)$ is a strictly decreasing function from $K(0) = \infty$ to $K(l) = 0$]; $K[\Xi_e^{-1}(ct_1)]$ will be the value of K leading to the specified inversion time t_1 . $T(\xi) \ll 1$ for small ξ and rapidly grows around ξ_1 . We choose ξ_1 so that $\xi_1 - \xi_0$ is positive, as small as possible, but makes $K(\xi_1)$ still compatible with (A6); this guarantees $\bar{t} \simeq t_0 \simeq \bar{t}_1$ and an efficient slingshot loading.

About the relativistic harmonic oscillator. Assuming for simplicity $\mathbf{u}_{e\perp} = 0$, from (7) we find that $\Delta z(t, Z) \equiv z_e(t, Z) - Z$ fulfills

$$\begin{aligned} 1 + 2K[\zeta^2 - \Delta z^2] &= \tilde{\gamma}_e = 1/\sqrt{1 - \tilde{\beta}_e^2} \quad \Rightarrow \\ \frac{1}{c} \frac{d\Delta z}{dt} &= \tilde{\beta}_e^z = -\frac{\sqrt{4K[\zeta^2 - \Delta z^2] + 4K^2[\zeta^2 - \Delta z^2]^2}}{1 + 2K[\zeta^2 - \Delta z^2]} \quad \Rightarrow \\ \Delta t &= \frac{1}{2c\sqrt{K}} \int_{\Delta z}^\zeta \frac{dy [1 + 2K(\zeta^2 - y^2)]}{\sqrt{\zeta^2 - y^2 + K(\zeta^2 - y^2)^2}} \end{aligned}$$

Therefore the time lapse Δt for the electrons to go from $z_e = Z + \zeta$ with zero initial velocity to $z_e = Z + \Delta z$ is

$$\Delta t = \frac{\zeta}{c} f\left(\frac{\Delta z}{\zeta}; K\zeta^2\right), \quad f(D; \chi) \equiv \int_D^1 \frac{dv [1/2 + \chi(1-v^2)]}{\sqrt{\chi} \sqrt{1-v^2 + \chi(1-v^2)^2}}, \quad (\text{A8})$$

$[\Delta z(t, Z)$ is independent of Z , and so is Δt]. In particular the time needed to return from $z = Z + \zeta$ to their initial equilibrium position $z = Z$ is, as claimed,

$$\frac{1}{4} T_H = \frac{1}{2c\sqrt{K}} \int_0^\zeta \frac{dz [1 + 2K(\zeta^2 - z^2)]}{\sqrt{\zeta^2 - z^2 + K(\zeta^2 - z^2)^2}}.$$

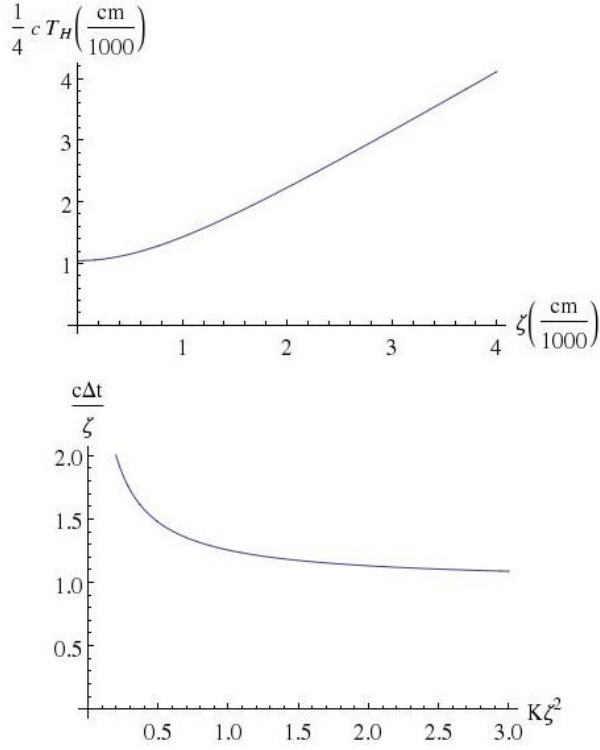


FIG. 6. The return time lapse $T_H/4$ for $K \equiv \pi e^2 n_0 / mc^2 = 5.7 \times 10^{-7} \text{cm}^{-2}$ as a function of the penetration ζ (up), the ratio $cT_H/4\zeta$ as a function of $K\zeta^2$ (down).

T_H is the plasma oscillation period. In fig. 6-up we plot $cT_H/4$ as a function of ζ for $K = 5.7 \times 10^{-7} \text{cm}^{-2}$ (a value relevant for a possible experiment at FLAME, see below) [23]. The ratio $cT_H/4\zeta$ is a function of $K\zeta^2$ only, going to 1 as $K\zeta^2 \rightarrow \infty$, see fig. 6-down, i.e. the average electron velocity goes to c in this limit. The function f defined in (A8) is a strictly decreasing, and therefore invertible, function of $D \in [-1, 1]$, and so is

$$m(D; \chi) \equiv f(D; \chi) - D.$$

Inverting (A8) at fixed $K\zeta^2$ we obtain $\Delta z = f^{-1}(c\Delta t/\zeta, K\zeta^2)$. Setting $\Delta t \equiv (t - \bar{t}) - Z/c$ we obtain $z_e(t, Z)$ in the backward motion of the electrons. (A8) is also equivalent to $m(\Delta z/\zeta; K\zeta^2) = c[(t - \bar{t}) - z]/\zeta$; inverting the latter we find $Z_e(t, z)$ in the backward motion.

The whole electron motion until expulsion.

Combining the last results with (A2) we obtain our basic approximation for the whole motion of the electrons until their expulsion in the plane wave idealization:

$$z_e(t, Z) = \begin{cases} ct - \Xi_e^{-1}(ct - Z) & t \leq \bar{t} + Z/c, \\ Z + \zeta f^{-1}\left\{\frac{c(t - \bar{t}) - Z}{\zeta}; K\zeta^2\right\} & t_e \geq t > \bar{t} + Z/c. \end{cases} \quad (\text{A9})$$

$$Z_e(t, z) = \begin{cases} z - Y_e^z(ct - z) & ct - z \leq \xi_0, \\ z - \zeta m^{-1}\left\{\frac{c(t - \bar{t}) - z}{\zeta}; K\zeta^2\right\} & ct - z > \xi_0. \end{cases} \quad (\text{A10})$$

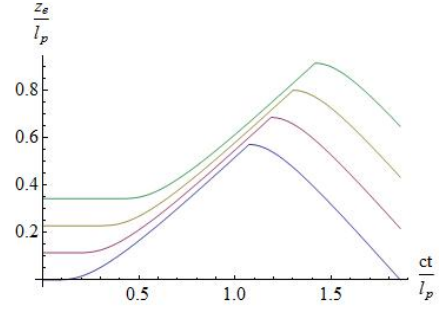


FIG. 7. The graphs of the function (A9) of t for the initial values $Z = 0, 0.2\zeta, 0.4\zeta, 0.6\zeta$ and other parameters (pulse length l_p , etc.) given in the central column of Table I.

In fig. (7) we plot the graphs of $z_e(\cdot, Z)$ (worldlines) normalized to l_p (the pulse length available at FLAME) for a few fixed values of Z ; these worldlines do not intersect, or equivalently the map $z \mapsto Z$ is one-to-one for each fixed t . Replacing $Z_e(t, z)$ in (A5) we find $n_e(t, z)$.

Appendix B: $R < \infty$ corrections to electron motions

Here we study where (A9) is a good approximation of the *real* electron motion induced by a pulse of *finite* R .

The general solution (retarded electromagnetic potential) of the Maxwell equation $\square A^\mu = 4\pi j^\mu$ in the Lorentz gauge ($\partial_\mu A^\mu = 0$) with zero asymptotic conditions reads

$$A^\mu(t, \mathbf{x}) = \int d^3x' \frac{j^\mu[t_r(x, \mathbf{x}'), \mathbf{x}']}{|\mathbf{x} - \mathbf{x}'|}, \quad t_r(x, \mathbf{x}') \equiv t - \frac{|\mathbf{x} - \mathbf{x}'|}{c}, \quad (\text{B1})$$

and $\mathbf{E}(t, \mathbf{x}) = -\frac{1}{c} \partial_t \mathbf{A} - \nabla A^0$. As a first rough approximation of the real current induced by the pump (1) we adopt

$$(j^\mu(t, \mathbf{x})) \equiv e \left(\widetilde{n}_{e0}(z) - n_e(t, z), -(n_e \boldsymbol{\beta}_e)(t, z) \right) \theta(R - \rho), \quad (\text{B2})$$

where $\widetilde{n}_{e0}(Z) = n_0 \theta(Z)$ and $n_e, \boldsymbol{\beta}_e$ are determined from (A5), (A9-A10); a plot of j^0 is in fig. 8. As velocities are relativistic, (B1) differs significantly from the instantaneous counterpart where t_r is replaced by t . It gives the EM potential (and field, after derivation) generated by the electric current (B2), which adds to the pump (1). We now estimate its influence over the electron motion (B2) itself, and where this can be neglected.

i) Determination of \widetilde{E}^z on the z -axis. Below we show that if $\widetilde{n}_{e0}(Z)$ vanishes at $Z < 0$ the condition

$$0 \leq z \leq ct \leq \sqrt{R^2 + z^2} \quad (\text{B3})$$

implies

$$E^z(t, z, \hat{\mathbf{z}}) = 4\pi e \{ \widetilde{N}_e(z) - \widetilde{N}_e[Z_e(t, z)] \}, \quad (\text{B4})$$

with $\widetilde{N}_e(Z) \equiv \int_0^Z dy \widetilde{n}_{e0}(y)$ a primitive of \widetilde{n}_{e0} . If $\widetilde{n}_{e0}(Z) = n_0 \theta(Z)$ then $\widetilde{N}_e(Z) = n_0 Z \theta(Z)$, and (B4) becomes (2),

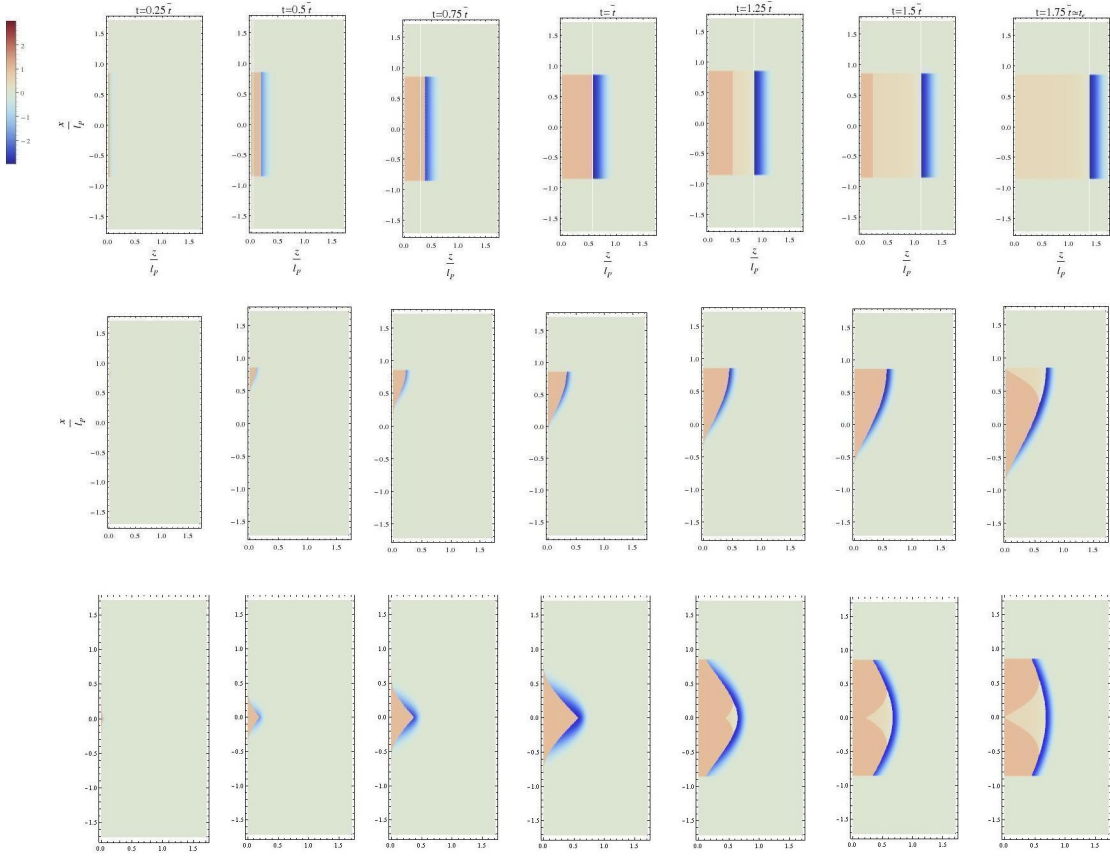


FIG. 8. Upper row: coloured plots in the z, x plane of the normalized charge density $\frac{j^0(t, z, x)}{en_0}$ multiplied by the characteristic function of the cylinder C_R , at $t=0.25\bar{t}, 0.5\bar{t}, 0.75\bar{t}, 1.25\bar{t}, 1.5\bar{t}, 1.75\bar{t}$ for the possible FLAME experiment parameters $R/\zeta = 1.5$, $K\zeta^2=0.654$; $j^0(t, z, x)$ is computed in the approximation (A9-A10). z, x are expressed in units of the length l_p of the pulse. We name $S_0(t)$ the surface of discontinuity between the positively (brown) and negatively (blue) charged region.

Central row: corresponding coloured plots of the retarded normalized charge density $\frac{j^0(t_r, z, x)}{en_0}$ ($t_r = t - |\mathbf{x} - \mathbf{x}'|/c$) at the same times, as seen from the point $\mathbf{x} = R\hat{\mathbf{x}}$ of ∂C_R .

Lower row: corresponding coloured plots of the retarded normalized charge density $\frac{j^0(t_r, z, x)}{en_0}$ ($t_r = t - |\mathbf{x}_e(t, \mathbf{0}) - \mathbf{x}'|/c$) at the same times, as seen from the point $\mathbf{x}_e(t, \mathbf{0}) = z_e(t, 0)\hat{\mathbf{z}}$ on the $\hat{\mathbf{z}}$ -axis.

exactly as in the $R = \infty$ case. This should not come as a surprise: (B3) ensures that the spacetime region where the $R < \infty$ and the $R = \infty$ 4-current j^μ differ is not causally connected to the spacetime point $(ct, z\hat{\mathbf{z}})$ [24].

Moreover, we show that $\widetilde{E}^z(t, Z\hat{\mathbf{z}})$ remains very close to the Lagrangian counterpart of (2) for a time lapse growing with R/ζ , even if the Lagrangian formulation of (B3), i.e. $0 \leq z_e(t, Z) \leq ct \leq \sqrt{R^2 + [z_e(t, Z)]^2}$, is not fulfilled. Tuning R/ζ we can thus neglect their difference until the expulsion time t_e . In particular we find that for the suggested experiments at FLAME $E^z(\bar{t}, \zeta\hat{\mathbf{z}})/4\pi en_0$ practically coincides with 1 with both choices $\sigma \equiv R/\zeta = 1.25, 1.5$.

We determine $\widetilde{E}^z(t, Z\hat{\mathbf{z}})$ first for a generic $\widetilde{n}_{e0}(Z)$ vanishing at $Z < 0$. Denoting the cylindrical coordinates of

\mathbf{x}' as (z', ρ, φ) , from (B1-B2) it follows

$$\begin{aligned} \frac{1}{2\pi e} E^z(t, z\hat{\mathbf{z}}) &= -\frac{1}{2\pi e} \left[\frac{1}{c} \partial_t A^z + \partial_z A^0 \right] \\ &= \int_0^{ct} \frac{d\varphi}{2\pi} \int_0^z dz' \int_0^R \rho d\rho \left\{ \frac{\partial_t (n_e \beta_e^z)(t_r, z')}{c\sqrt{(z-z')^2 + \rho^2}} - \partial_z \frac{\widetilde{n}_{e0}(z') - n_e(t_r, z')}{\sqrt{(z-z')^2 + \rho^2}} \right\} \\ &= \int_0^{ct} dz' \int_0^R d\rho \partial_\rho \left\{ \frac{(z-z')[n_e(t_r, z') - \widetilde{n}_{e0}(z')]}{\sqrt{(z-z')^2 + \rho^2}} - (n_e \beta_e^z)(t_r, z') \right\} \\ &= \int_0^{ct} dz' \left\{ \frac{(z-z')[n_e(t_r, z') - \widetilde{n}_{e0}(z')]}{\sqrt{(z-z')^2 + \rho^2}} - (n_e \beta_e^z)(t_r, z') \right\}_{\rho=0}^{\rho=R} \end{aligned}$$

$$\begin{aligned}
&= \int_0^{ct} dz' \left\{ \frac{(z-z') \{ [\widetilde{n}_{e0}(Z_e) \partial_y Z_e](ct_r, y) \Big|_{y=z'} - \widetilde{n}_{e0}(z') \}}{\sqrt{(z-z')^2 + \rho^2}} \right. \\
&\quad \left. + \frac{1}{c} [\widetilde{n}_{e0}(Z_e) \partial_t Z_e](t_r, z') \right\}_{\rho=0}^{\rho=R}; \quad (\text{B5})
\end{aligned}$$

in the derivation we have used: $ct_r = ct - \sqrt{(z-z')^2 + \rho^2}$ for $\mathbf{x} = z\hat{z}$; for any differentiable function $f(s)$ the identities $\rho \partial_z f[t_r] = \partial_\rho(z-z')f(t_r)$, $\frac{-\rho}{c\sqrt{(z-z')^2 + \rho^2}} \partial_t f(t_r) = \partial_\rho f(t_r)$; (A5) in the last equality. If $\widetilde{n}_{e0}(Z) = n_0\theta(Z)$ we find

$$\begin{aligned}
\frac{E^z(t, z\hat{z})}{2\pi en_0} &= \sqrt{(z-ct)^2 + R^2} - \sqrt{z^2 + R^2} - |z-ct| + |z| \quad (\text{B6}) \\
&+ \int_0^{ct} dz' \left\{ \frac{(z-z') [\theta(Z_e) \partial_y Z_e](t_r, y) \Big|_{y=z'}}{\sqrt{(z-z')^2 + \rho^2}} + \frac{\theta(Z_e) \partial_t Z_e(t_r, z')}{c} \right\}_{\rho=0}^{\rho=R}.
\end{aligned}$$

For the suggested FLAME experiment the numerical evaluation by *Mathematica* in the approximation (A1-A4), (A9-A10) gives $E^z(\bar{t}, \zeta\hat{z})/4\pi en_0 = .999$, $E^z(\bar{t}, \zeta\hat{z})/4\pi en_0 = 1$, respectively for $\sigma \equiv R/\zeta = 1.25$, $\sigma \equiv R/\zeta = 1.5$. as claimed after equation (B4).

Proof of (B4). In (B5) it is $t_r = t - \sqrt{R^2 + (z-z')^2}$ for $\rho = R$; from (B3) and $z' \geq 0$ it follows $ct_r \leq z'$ [25], whence $z_e(t_r, Z) = Z$, $Z_e(t_r, z') = z'$, $\partial_{z'} Z_e(t_r, z') = 1$, $\partial_t Z_e(t_r, z') = 0$, so that the integrand in (B5) vanishes for $\rho = R$. For $\rho = 0$ it is $t_r = t - |z' - z|/c$, and (B5) gives

$$\begin{aligned}
\frac{E^z(t, z\hat{z})}{2\pi e} &= \int_0^{ct} dz' \left[s(z, z') \{ [\widetilde{n}_{e0}(Z_e) \partial_y Z_e](t - |z' - z|/c, y) \Big|_{y=z'} \right. \\
&\quad \left. - \widetilde{n}_{e0}(z') \} - \frac{1}{c} [\widetilde{n}_{e0}(Z_e) \partial_t Z_e](t - |z' - z|/c, z') \right] \\
&= \int_0^{ct} dz' s(z, z') \left\{ \widetilde{n}_{e0}(Z_e) \partial_{z'} [Z_e(t - |z' - z|/c, z')] - \widetilde{n}_{e0}(z') \right\} \\
&= \int_0^{ct} dz' s(z, z') \left\{ \partial_{z'} \widetilde{N}_e [Z_e(t - |z' - z|/c, z')] - \widetilde{n}_{e0}(z') \right\} \\
&= \int_z^{ct} dz' \left\{ \partial_{z'} \widetilde{N}_e [Z_e(t + (z - z')/c, z')] - n_{e0}(z') \right\} \\
&\quad - \int_0^z dz' \left\{ \partial_{z'} \widetilde{N}_e [Z_e(t + (z' - z)/c, z')] - \widetilde{n}_{e0}(z') \right\} \\
&= \widetilde{N}_e \left[Z_e \left(\frac{z}{c}, ct \right) \right] - \widetilde{N}_e(ct) + 2 \left\{ \widetilde{N}_e(z) - \widetilde{N}_e [Z_e(t, z)] \right\} \\
&+ \widetilde{N}_e \left[Z_e \left(t - \frac{z}{c}, 0 \right) \right] = 2 \left\{ \widetilde{N}_e(z) - \widetilde{N}_e [Z_e(t, z)] \right\} \quad (\text{B7})
\end{aligned}$$

where $s(z, z')$ stands for the sign of $z' - z$; in the last equality we have used $Z_e(z/c, ct) = ct > 0$, $Z_e(t, z) > 0$, $Z_e(t - z/c, 0) < 0$, $\widetilde{N}_e [Z_e(t - z/c, 0)] = 0$. Note that the condition $ct_r \leq z'$ is equivalent to requiring that t is less than the sum of the time necessary for the pulse to reach any point $\mathbf{x}' \in \partial C_R$ and of the time lapse necessary for a EM signal to travel from \mathbf{x}' to $\mathbf{x} = z\hat{z}$, what ensures by causality also that at such t the fields in \mathbf{x} have not been influenced by the plasma outside ∂C_R , as anticipated.

ii) Upper bound for \widetilde{E}^ρ and for the inner displacement of the electrons outside C_R . As our goal here is to find a sufficient condition for a significant expulsion (expulsion for all electrons initially located in C_r , $r \gtrsim R/2$, say), for simplicity of computations we overestimate the σ of eq. (8) as follows. For all electrons initially located at points $\mathbf{X} \simeq R\hat{\rho} + Z\hat{z}$ (with some unit vector $\hat{\rho} \equiv \cos \Phi \hat{x} + \sin \Phi \hat{y}$) around the lateral boundary ∂C_R of C_R we: a) neglect the initial outward boost induced by the pulse on them; b) overestimate the inward component $e\widetilde{E}^\rho(t, \mathbf{X}) \equiv eE^\rho[t, \mathbf{x}_e(\mathbf{X})]$ of the electric force exerted on them by the charge distribution within C_R , and consequently their inward displacement $|\Delta\rho_e|$, by the upper bound $E^\rho(t, R\hat{\rho})$ [26]; c) overestimate $1/\widetilde{\gamma}_e = 1/\sqrt{1 + \widetilde{\mathbf{u}}_e^2}$ by $1/\sqrt{1 + \widetilde{u}_e^2}$ in their relativistic equation of motion. We show that for t in a time lapse growing with σ

$$\mathbf{E}(t, \mathbf{x}) \simeq E^\rho(t, \mathbf{x})\hat{\rho} + E^z(t, \mathbf{x})\hat{z}, \quad E^\rho(t, \mathbf{x}) \ll \widetilde{E}^z(t, \mathbf{0}) \quad (\text{B8})$$

on all points $\mathbf{x} \in \partial C_R$, i.e. there the electric field is essentially in the ρ -direction and much less than the longitudinal one experienced by the $\mathbf{X} = \mathbf{0}$ electrons. This is due to geometrical reasons (a look at the coloured charge density plot of fig. 8 center and down may help in getting a qualitative understanding): on one hand, to the delay inherent to the retarded potential itself; on the other, to the fact that the contributions generated by the ions and by the forward boosted electrons sum up on their surface $S_0(t)$ of separation, while they partially cancel on ∂C_R . Therefore tuning σ we can make $|\Delta\rho_e(t_e, R\hat{\rho} + z\hat{z})| \leq R - r$ for all z , i.e. the inward displacement of all surface electrons at the estimated time of expulsion $t_e = \bar{t} + \Delta t$ small enough not to obstruct the way out to the electrons within C_r . In particular we find that for the suggested experiments at FLAME it is sufficient to choose $\sigma \equiv R/\zeta = 1.25$, 1.5 to respectively obtain $r/R \geq 1/2$, $2/3$.

For circular polarization E^ρ , \widetilde{E}^ρ are strictly the same on all the points of this circle $\rho = R$, $z = 0$, in particular on the point $\mathbf{x} = R\hat{x}$: $E^\rho(t, R\hat{x}) = E^x(t, R\hat{x})$. For other (in particular linear) polarizations the relative variation of E^ρ , \widetilde{E}^ρ along the circle is negligible for modulated periodic oscillations, since the charge distribution has almost cylindrical symmetry due to the fact that transverse displacements almost average to zero in each cycle; therefore also in this case $E^\rho(t, R\hat{x}) \simeq E^x(t, R\hat{x})$. By (B1-B2)

$$\begin{aligned}
E^x(t, x\hat{x}) &= -\frac{1}{c} \partial_t A^x - \partial_x A^0 \\
&= e \int_0^{2\pi} d\varphi \int_0^{ct} dz \int_0^R \rho d\rho \left\{ \frac{\partial_t (n_e \beta_e^x)(t_r, z)}{c\sqrt{z^2 + C}} - \partial_x \frac{n_0 - n_e(t_r, z)}{\sqrt{z^2 + C}} \right\} \\
&= e \int_0^{2\pi} d\varphi \int_0^{ct} dz \int_0^R \rho d\rho \left\{ \frac{\partial_t (n_e \beta_e^x)(t_r, z) + c \partial_x n_e(t_r, z)}{c\sqrt{z^2 + C}} \right. \\
&\quad \left. + \frac{[n_0 - n_e(t_r, z)](x - \rho \cos \varphi)}{|z^2 + C|^{3/2}} \right\} \quad (\text{B9})
\end{aligned}$$

where $C = x^2 + \rho^2 - 2x\rho \cos \varphi$, $ct_r = ct - \sqrt{z^2 + C}$ for $\mathbf{x} = x\hat{x}$.

	$R/\zeta=1.25$	$R/\zeta=1.5$
$ \beta_e^\rho(\bar{t}, R\hat{\rho}) $	< 0.154	< 0.136
$ \widetilde{\Delta\rho}_e(\bar{t}, R\hat{\rho}) /R$	< 0.059	< 0.04
average $\tilde{\beta}_e^\rho$ in $[0, \bar{t}]$	$\simeq 0.041$	$\simeq 0.03$
$ \beta_e^\rho(t_e, R\hat{\rho}) $	< 0.7	< 0.58
$ \widetilde{\Delta\rho}_e(t_e, R\hat{\rho}) /R$	< 0.50	< 0.33
average $\tilde{\beta}_e^\rho$ in $[\bar{t}, t_e]$	< 0.43	< 0.32

TABLE II. Main outputs of the inward motion of the lateral electrons in the proposed FLAME experiments

Replacing the approximated Z_e (A10) in (A5) and the resulting densities in eq. (B9), integrating the relativistic

equations of motion of the electron $-e\widetilde{E}^x = d\widetilde{p}_e^x/dt = mcd\widetilde{u}_e^x/dt$, $dx_e/dt = c\widetilde{\beta}_e^x = c\widetilde{u}_e^x/\widetilde{\gamma}_e$ with initial conditions $\widetilde{p}_e^x(0, x\hat{x}) = 0$, $x_e(0, x\hat{x}) = x\hat{x}$ ($x \geq R$), using overestimates b), c) and *Mathematica* we numerically find the bounds of table II for $\widetilde{\beta}_e^\rho(\bar{t}, R\hat{\rho})$, $\widetilde{\Delta\rho}_e(t, R\hat{\rho}) = \Delta x_e(t, R\hat{x})$ in the suggested FLAME experiments.

Finally, we argue that if in (1) we replace $\theta(R-\rho)$ by $e^{-\rho^2/R^2}$, then outer electrons cause a smaller obstruction to the expulsion of the $\mathbf{X} \sim \mathbf{0}$ electrons. In fact, also the outer electrons with initial $\rho \geq R$ get some displacement $\Delta z > 0$, therefore (attracted by the ions) cover a smaller inward distance $\Delta\rho_e$ in the time necessary for the $\mathbf{X} \sim \mathbf{0}$ electrons to come back to $\mathbf{x} \sim (0, 0, \Delta z)$, and therefore cannot intercept those in a larger cylinder C_r .

- [1] T. Tajima, J.M. Dawson, *Phys. Rev. Lett.* **43** (1979), 267.
[2] L.M. Gorbunov, and V.I. Kirsanov, *Sov. Phys. JETP* **66**, 290 (1987).
[3] P. Sprangle, E. Esarey, A. Ting, and G. Joyce, *Appl. Phys. Lett.* **53**, 2146 (1988).
[4] A. Irman, M.J.H. Luttikhof, A.G. Khachatryan, F.A. van Goor, J.W.J. Verschuur, H.M.J. Bastiaens, K.-J. Boller, *J. Appl. Phys.* **102** (2007), 024513.
[5] C. Joshi, *Scientific American* **294** (2006), 40.
[6] J. Faure, Y. Glinec, A. Pukhov, S. Kiselev, S. Gordienko, E. Lefebvre, J.-P. Rousseau, F. Burgy, V. Malka, *Lett. Nat.* **431**, 541544 (2004).
[7] S. Kalmykov, S. A. Yi, V. Khudik, and G. Shvets, *Phys. Rev. Lett.* **103** (2009), 135004.
[8] X. Wang, *et al.*, *Nature Communications* **4** (2013), 1988.
[9] G. Fiore, *J. Phys. A: Math. Theor.* **47** (2014), 225501.
[10] G. Fiore, *Acta Appl. Math.* **132** (2014), 261-271.
[11] L.A. Gizzi, *et al.*, *Appl. Sci.*, **3** (2013), 559-580; doi:10.3390/app3030559.
[12] L. Pribyl, L. Juha, G. Korn, *et al.*, in Proc. IBIC2012, Tsukuba, Japan (2012), pp. 482485.
[13] V.I. Eremin, A.V. Korzhimanov, A.V. Kim, *Phys. Plasmas* **17** (2010), 043102.
[14] J.P. Geindre, R.S. Marjoribanks, P. Audebert, *Phys. Rev. Lett.* **104** (2010), 135001.
[15] A.A. Gonoskov, A.V. Korzhimanov, A.V. Kim, M. Marklund, A.M. Sergeev, *Phys. Rev.* **E84** (2011), 046403.
[16] $\tau = \tau_1 + \tau_2$, with τ_1, τ_2 the time lapses spent during the oscillation respectively in the domain of the elastic and of the constant force; due to the size of the domains it is $\tau_1 \geq T_H^{nr}/2$. Hence τ depends on Z and on the oscillation amplitude, but is at the least of the order of T_H^{nr} .
[17] The longitudinal eq. of motion of the $Z=0$ electrons is

$$\frac{d\widetilde{p}_e^z}{dt} = m[F_p^z(ct - z_e) - \omega_p^2 z_e], \quad F_p^z(\xi) \equiv \frac{(e\lambda)^2 \eta \partial_\xi \epsilon_s^2(\xi)}{8(m\pi)^2 c^3 \gamma(\xi)},$$

where $\eta = 1, 1/2$ respectively for circular, linear polarization, and $\omega_p^2 = 4\pi e^2 n_0/m$ is the square of the plasma frequency. In the nonrelativistic regime we find $\widetilde{\gamma} \simeq 1$, $z_e(t) \ll ct$, $\widetilde{p}_e^z \simeq m\dot{z}_e$, hence the maximum of $\epsilon_s^2(\xi)$ and the end of the pulse reach these electrons respectively at $t \simeq \bar{t} = \xi_0/c$, $t \simeq l/c$, and the equation of motion in

the bulk reduces to that of a forced harmonic oscillator: $\ddot{z}_e = F_p^z(ct) - \omega_p^2 z_e$; the solution with initial conditions $z_e(0) = \dot{z}_e(0) = 0$ is $z_e(t) = \int_0^t dt' F_p^z(ct') \sin[\omega_p(t-t')]/\omega_p$. Electrons initially located at small $Z > 0$ will experience approximately the same longitudinal displacement with a time delay Z/c . $\widetilde{F}_p^z \widetilde{v}^z = F_p^z \dot{z}_e$ keeps nonnegative if during the pulse $\dot{z}_e(t) = \int_0^t dt' F_p^z(ct') \cos[\omega_p(t-t')]$ switches from positive to negative at $t = \bar{t} = \xi_0/c$ (only). In particular it must be $z_e(t) \geq 0$ for all $t \leq l/c$, and ξ_0, n_0, l must fulfill $\pi/4 < \xi_0 \omega_p/c < 3\pi/4$.

If the pulse is so intense to make electrons relativistic the conditions for maximal slingshot loading are more complicated; for an estimate in the proposed experimental conditions see the comments after (A7).

- [18] In (6) we have chosen the additive constant so that the minima of U w.r.t. z_e are equal to zero for all Z .
[19] To perform the work integral we have used the relation $\sqrt{z^2 + R^2} = \frac{1}{2} \partial_z [z\sqrt{z^2 + R^2} + R^2 \sinh^{-1} \frac{z}{R}]$. We have chosen the additive constant equal to the last three terms so that $U_R(0^-, Z) = U(0^+, Z)$.
[20] D. Jovanović, R. Fedele, F. Tanjia, S. De Nicola, L. A. Gizzi, *Eur. Phys. J.* **D66** (2012), 328.
[21] A. Pukhov, *Rep. Prog. Phys.* **65** (2002), R1-R55.
[22] W. Lu, M. Tzoufras, C. Joshi, F. S. Tsung, J. Vieira, R. A. Fonseca, L. O. Silva, *Phys. Rev. ST Accel. Beams* **10** (2007), 061301.
[23] As $\partial T_H / \partial \zeta|_{\zeta=0} = 0$, only in the nonrelativistic limit $T_H \stackrel{\zeta \rightarrow 0}{\simeq} T_H^{nr} = \pi/c\sqrt{K} = \sqrt{\pi m/e^2 n_0}$ is independent of ζ (nonrelativistic harmonic oscillator).
[24] In fact, (B3) implies $t < (z' + |\mathbf{x} - \mathbf{x}'|)/c$ for all $\mathbf{x}' \notin C_R$; z'/c is the time when the $R = \infty$ pulse reaches \mathbf{x}' , $|\mathbf{x} - \mathbf{x}'|/c$ is the time lapse necessary for a EM signal to travel from \mathbf{x}' to \mathbf{x} , hence their sum is the time when the information that the charge distribution does not extend indefinitely in the xy plane, but is confined in C_R , arrives at \mathbf{x} .
[25] In fact, by the assumptions we find $-2ctz' \leq -2zz'$, $(ct - z')^2 = (ct)^2 - 2ctz' + z'^2 \leq R^2 + z^2 - 2zz' + z'^2 = R^2 + (z - z')^2$ and, taking the square root, $ct_r \leq z'$.
[26] In fact, eE^p decreases as Z grows and when the electrons penetrate inside C_R , as correspondingly the negative contribution due to the electrons displaced beyond $S_0(t)$ grows, while the positive one by the ions decreases.